

Structural basis of histone demethylation by LSD1 revealed by suicide inactivation

Maojun Yang^{1,4}, Jeffrey C Culhane^{2,4}, Lawrence M Szewczuk^{2,4}, Christian B Gocke¹, Chad A Brautigam³, Diana R Tomchick³, Mischa Machius³, Philip A Cole² & Hongtao Yu¹

Histone methylation regulates diverse chromatin-templated processes, including transcription. The recent discovery of the first histone lysine-specific demethylase (LSD1) has changed the long-held view that histone methylation is a permanent epigenetic mark. LSD1 is a flavin adenine dinucleotide (FAD)-dependent amine oxidase that demethylates histone H3 Lys4 (H3-K4). However, the mechanism by which LSD1 achieves its substrate specificity is unclear. We report the crystal structure of human LSD1 with a propargylamine-derivatized H3 peptide covalently tethered to FAD. H3 adopts three consecutive γ -turns, enabling an ideal side chain spacing that places its N terminus into an anionic pocket and positions methyl-Lys4 near FAD for catalysis. The LSD1 active site cannot productively accommodate more than three residues on the N-terminal side of the methyllysine, explaining its H3-K4 specificity. The unusual backbone conformation of LSD1-bound H3 suggests a strategy for designing potent LSD1 inhibitors with therapeutic potential.

Covalent modifications of histone tails, such as lysine methylation, regulate various biological processes that require access to genomic DNA in the context of chromatin^{1,2}. The recent discovery of the first histone lysine-specific demethylase, LSD1, establishes the reversible nature of histone methylation and indicates that these epigenetic marks are actively removed depending on context and at specific genomic loci^{3,4}. LSD1 belongs to the amine oxidase superfamily of FAD-dependent enzymes^{3,4}. It is a component of transcriptional repressor complexes and specifically removes mono- and dimethylation on H3-K4 in an FAD-dependent amine oxidation reaction^{3,4}. By reducing FAD to FADH₂, LSD1 oxidizes the methyl ϵ -amine of lysine to form an imine intermediate that is hydrolyzed to produce formaldehyde and the demethylated lysine. FADH₂ is then oxidized by molecular oxygen to regenerate FAD in a reaction that also produces H₂O₂. Owing to the inherent limitations of this chemistry, LSD1 can only demethylate mono- and dimethylamines that contain a lone pair of electrons in their deprotonated state. LSD1, on its own, specifically demethylates mono- and dimethylated H3-K4, but not other methylated lysines in core histones, although there is evidence to suggest that binding of other factors enables LSD1 to demethylate histone H3 Lys9 (H3-K9), thus activating transcription^{5–7}. We and others have recently determined crystal structures of LSD1, either alone or in complex with a fragment of the corepressor protein CoREST^{8–10}. However, none of the structures have contained an H3 peptide substrate. Thus, how LSD1 achieves its site specificity toward H3-K4 is unknown. In this study, we covalently tethered a methyl-Lys4-containing H3 peptide to

the FAD cofactor of human LSD1 through the use of a suicide inactivator and determined the crystal structure of the resulting complex. This suggests a straightforward explanation for the H3-K4 specificity of LSD1 and provides a basis for testing of the proposed interactions in this and future studies.

RESULTS

Structure determination of LSD1–CoREST–H3

Our repeated efforts to cocrystallize LSD1–CoREST with a dimethylated H3-K4 peptide failed to produce visible electron density for the peptide, presumably owing to the weak and/or transient nature of the LSD1–H3 interaction ($K_m = 39 \mu\text{M}$; **Supplementary Table 1** online). Covalent tethering of substrates to enzymes or cofactors has proven to be an effective strategy for capturing transient enzyme–substrate complexes and enabling their structural characterization^{11,12}. Along these lines, we have previously shown that propargylamine-derivatized peptides containing the N-terminal 21 residues of H3 (propargyl-K4 H3_{1–21}) are mechanism-based inactivators of LSD1 that ultimately form a covalent linkage with FAD¹³. Furthermore, we have deduced the chemical structure of the covalent adduct between FAD and propargyl-K4 H3_{1–21} using optical and NMR spectroscopy¹⁴. Because an additional covalent linkage between FAD and the H3 peptide would presumably increase the peptide occupancy in the LSD1 active site, we grew crystals with LSD1–CoREST treated with propargyl-K4 H3_{1–21}. However, these crystals still did not produce electron density belonging to the H3 peptide, suggesting that the covalent adduct was

¹Department of Pharmacology, The University of Texas Southwestern Medical Center, 6001 Forest Park Road, Dallas, Texas 75390, USA. ²Department of Pharmacology and Molecular Sciences, Johns Hopkins University School of Medicine, Baltimore, Maryland 21205, USA. ³Department of Biochemistry, The University of Texas Southwestern Medical Center, 5323 Harry Hines Boulevard, Dallas, Texas 75390, USA. ⁴These authors contributed equally to this work. Correspondence should be addressed to P.A.C. (pcole@jhmi.edu) or H.Y. (hongtao.yu@utsouthwestern.edu).

Received 21 March; accepted 26 April; published online 27 May 2007; doi:10.1038/nsmb1255

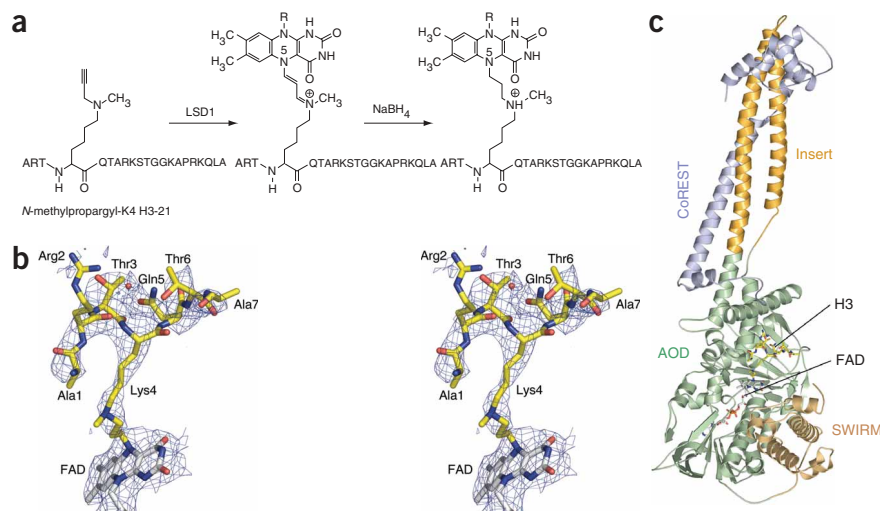


Figure 1 Structure of LSD1–CoREST bound to a derivatized histone H3 tail. **(a)** Chemical structures of *N*-methylpropargyl-K4 H3_{1–21}, its covalent adduct with FAD, and the NaBH₄-reduced adduct. **(b)** Stereo view of the structure of the *N*-methylpropargyl-K4 H3_{1–21}–FAD adduct in stick representation, overlaid with a simulated-annealing composite-omit map contoured at 1.2 σ . **(c)** Overall structure of LSD1–CoREST–H3. The FAD–H3 adduct is shown in stick representation. All structural figures were generated with PyMOL (<http://pymol.sourceforge.net>).

either unstable or heterogeneous under our crystallization conditions. We discovered that an *N*-methylpropargyl-K4 H3_{1–21} compound inhibited LSD1 five-fold more potently, with a K_i of 120 nM (Fig. 1a and Supplementary Figs. 1–4 online)¹⁴. This compound formed a covalent adduct with FAD and inhibited LSD1 in a time-dependent manner (Supplementary Figs. 1–4). According to mass spectrometry, the vast majority of the covalent adducts retained the methyl group on Lys4 (Supplementary Fig. 3). We thus incubated LSD1–CoREST with *N*-methylpropargyl-K4 H3_{1–21} (Fig. 1a) to form the FAD-peptide adduct. After inactivation, NaBH₄ was added to the mixture to reduce the double bonds in the linkage between the N5 atom of FAD and the N ϵ atom of the propargylamine inactivator, yielding a more homogeneous complex (Fig. 1a).

The structure of the LSD1–CoREST–H3 complex was then determined by X-ray crystallography to a resolution of 2.7 Å. Strong electron density was observed for residues 1–7 of H3, including the methyl-Lys4 side chain (Fig. 1b). There was indistinct electron density corresponding to the C-terminal portion of H3, which was therefore not included in the structure. Our structure of LSD1–CoREST–H3 (Fig. 1) provides an explanation for the H3–K4 specificity of LSD1 and reveals an elegant mode of molecular recognition that allows LSD1 to position the methyllysine side chain near the FAD while accommodating the residues on the N-terminal side of Lys4 in a deep active site cavity (Fig. 2).

The N terminus-binding pocket of LSD1

LSD1 consists of an N-terminal SWIRM domain and a C-terminal amine oxidase domain (AOD) that contains an insert (Fig. 1c). The insert forms two antiparallel helices that interact with CoREST. Binding of the derivatized H3 peptide does not appreciably alter the conformation of LSD1–CoREST, indicating that the active site cavity of LSD1 is preformed. Residues 1–7 of H3 fit snugly into this cavity (Fig. 2a), forming extensive, principally electrostatic and hydrogen-bonding interactions with FAD and a large set of active site residues of LSD1 (Fig. 2b). Ala1 of H3 inserts into an anionic pocket comprised of Asn540, Trp552, Asp555 and Asp556, with the N-terminal amine forming a hydrogen bond and an electrostatic interaction with Asp555 (Fig. 2a,b and Fig. 3a). The *N*-methylamine moiety of H3–K4 lies directly above the reduced isalloxazine ring of FAD (Fig. 2b). This binding mode, which imposes steric constraints on the H3 N terminus and requires the methyllysine to be positioned near FAD, dictates that

there cannot be more than three residues on the N-terminal side of the methyllysine. Such an H3-binding mode of LSD1 would readily explain its H3–K4 specificity. The distance between N ϵ of the modified H3–K4 and N5 of FAD is 4.9 Å. In a productive enzyme–substrate complex, it is possible that the

The unusual backbone conformation of H3

formally positive N ϵ group of methylated H3–K4 engages in cation– π interactions with the isalloxazine ring of FAD, thus bringing N ϵ closer to FAD and into a more optimal position for oxidation. Though the H3-binding mode observed in our structure is inconsistent with demethylation of H3–K9 by LSD1, we cannot exclude the possibility that, upon association with other proteins, LSD1 can develop other modes of substrate binding.

The LSD1–H3 interactions involving the N-terminal amine and methyllysine are reminiscent of those observed in several types of methylated H3–K4-binding domains², such as the PHD finger (Fig. 2c). In that case, the N-terminal amine of Ala1 of H3 also interacts with a negatively charged residue, whereas the trimethyllysine (H3K4me3) inserts into a cage formed by four aromatic residues, engaging in cation– π interactions². However, there is a notable difference between the binding modes of H3 in LSD1 and in all other methylated H3–K4-binding modules. The H3 peptide, when bound to other methylated H3–K4-binding domains, adopts an extended conformation and, in most cases, extends the existing β -sheet of its receptor² (Fig. 2c,d). In contrast, as necessitated by the deep active site cavity of LSD1, residues 2–6 of the H3 peptide bound to LSD1 adopt three consecutive γ -turns, with the carbonyl of residue *i* forming a hydrogen bond with the amide of residue *i* + 2 (Fig. 2e). As a result, the backbone of LSD1-bound H3 is severely compressed and has a serpentine shape (Fig. 2e,f), maximizing interactions between its side chains and active site residues of LSD1 (Fig. 3). The electron density for the Arg2 side chain of H3 is weak, but it is in the vicinity of Asp556, forming an ionic interaction (Fig. 3a). The aliphatic portion of the Arg2 side chain of H3 also contacts Trp552 of LSD1. Thr3 of H3 contacts Asn535 of LSD1. The methyl group of the covalently tethered H3–K4 forms hydrophobic interactions with Tyr761, Ala809 and Thr810 (Fig. 3b), consistent with the observation that *N*-methylpropargyl-K4 H3_{1–21} is a more potent LSD1 inhibitor than propargyl-K4 H3_{1–21}. The side chain and backbone carbonyl groups of Gln5 in H3 form hydrogen bonds with the side chain amide groups of Asn535 and Gln358 in LSD1, respectively (Fig. 3c). As revealed by the sequence alignment of residues surrounding the known methylation sites on histones (Fig. 3d), these sequence-specific interactions involving Arg2, Thr3 and Gln5 of H3 are expected to contribute to the substrate specificity of LSD1 toward H3–K4.

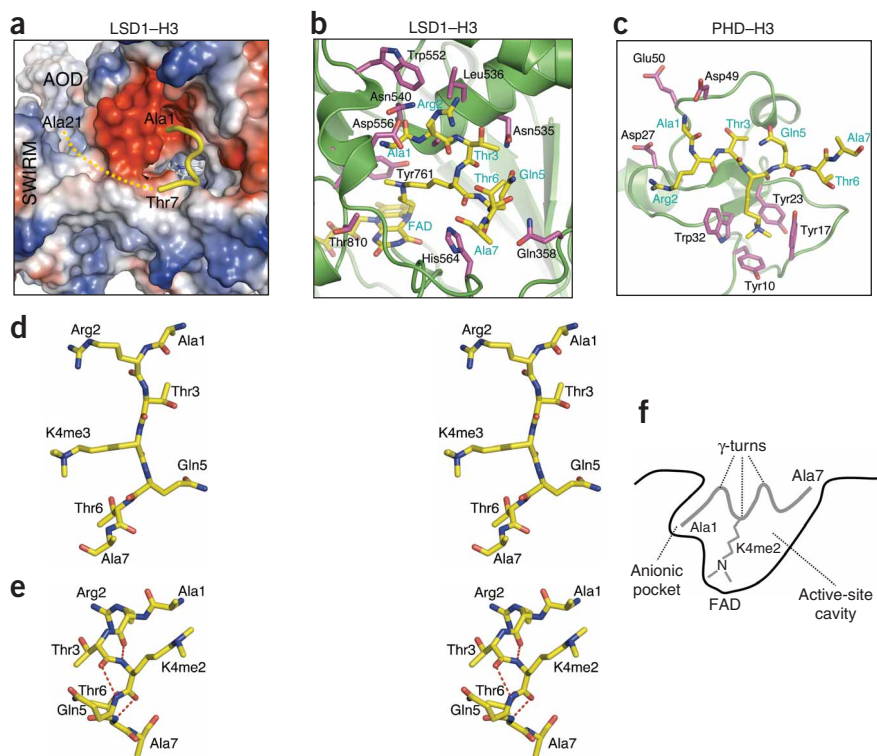


Figure 2 LSD1-bound H3 adopts an unusual backbone conformation. **(a)** Residues 1–7 of the H3 peptide (yellow tube) interact with the active site cavity of LSD1. Molecular surface of LSD1 AOD and SWIRM is colored by electrostatic potential: red, negative; blue, positive. Dashed yellow line represents C-terminal portion of H3, which might bind at a surface groove between AOD and SWIRM, according to existing biochemical evidence^{8,9}. **(b)** Binding of H3 at the active site of LSD1. Yellow, H3; purple, LSD1. **(c)** Binding of an H3K4me3 peptide to the PHD finger of BPTF (PDB 2FUU). Color scheme is as in **b**. **(d)** Stereo view of an H3K4me3 peptide bound to the PHD finger of ING2 (PDB 2G6Q). The distance between the C α atoms of Arg2 and Thr6 is 13.1 Å. **(e)** Stereo view of the derivatized H3 peptide bound to LSD1 (same scale as **e**). Dashed red lines represent the hydrogen bonds of the three γ -turns. The distance between the C α atoms of Arg2 and Thr6 is 9.2 Å. **(f)** Schematic drawing of interactions between LSD1 and the H3 peptide, highlighting the anionic pocket and the serpentine H3 backbone conformation that results from the three γ -turns.

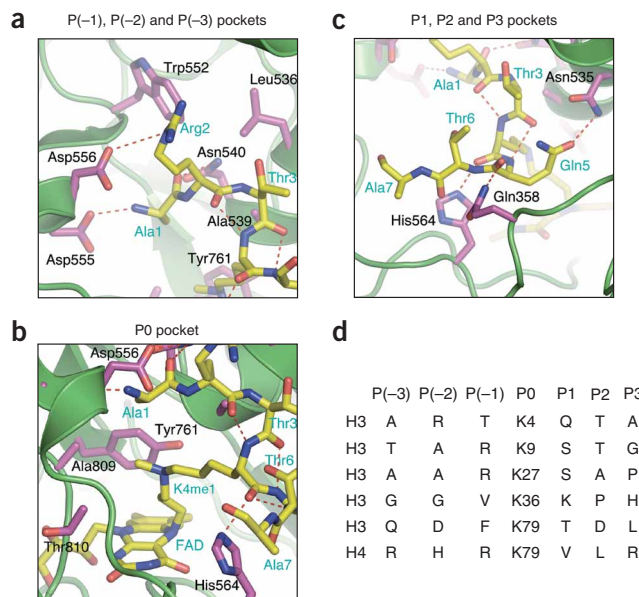
K4me2) (Supplementary Table 1). With the exception of Gln358, mutations of other H3-binding residues that directly contact H3, including Leu536, Asn540, Trp552 and His564, either substantially weakened or abolished the activity of LSD1. Correspondingly, mutation of Arg2 in H3 also abolished the activity, whereas mutation of Gln5 reduced the k_{cat}/K_m ratio by nine-fold. Notably, neutralization of the positive charge of the N terminus by acetylation (*N*-Ac-H3_{1–21}K4me2) or by replacing the N-terminal amino group with a methyl group (A1ibu-H3_{1–21}K4me2) reduced k_{cat}/K_m 99-fold or 23-fold, respectively. This is attributable to the essential role of the electrostatic interactions between the N terminus and Asp555, the stringent steric constraints of the anionic N terminus-binding pocket, or both. Furthermore, addition of a glycine at the

Mutagenesis analysis of LSD1 and H3

Our structural analysis of the LSD1-H3 interaction is consistent with previous biochemical studies^{9,10,15}. Notably, mutations of Asp555 and Asp556 that participate in favorable electrostatic interactions with the N terminus and Arg2 of H3, respectively, reduce the activity of LSD1 to less than 5% of that of the wild-type enzyme^{9,10}. Tyr761 and Asn535 interact with the H3-K4 methyl group and the side chain of Gln5 in H3; mutating these residues also substantially diminishes the activity of LSD1 (refs. 9,10). Finally, LSD1 recognizes an unusually large segment of the H3 tail and does not demethylate substrates containing fewer than 16 residues efficiently¹⁵. Though only the N-terminal seven residues of H3 are well ordered in our structure, the orientation of the H3 peptide is consistent with binding of its C-terminal portion into the groove between the SWIRM and AOD domains of LSD1, as implied by previous studies^{8,9}. There is precedent for observing only a subset of residues of a bound substrate in crystal structures, even though a longer peptide is required for efficient catalysis in solution. For example, residues 1–15 of histone H3 are required for efficient methylation by the DIM-5 H3-K9 methyltransferase, but only residues 8–12 are ordered in the crystal structure of the DIM-5-H3 complex¹⁶.

We further validated the molecular interactions between LSD1 and the derivatized H3 peptide observed in our structure by additional mutagenesis studies on both LSD1 and an H3 peptide substrate containing the N-terminal 21 residues and dimethyl-Lys4 (H3_{1–21}

Figure 3 Interactions between LSD1 and H3. **(a)** The binding pocket for Ala1, Arg2 and Thr3 of H3 (numbered P(-1), P(-2) and P(-3) relative to the modified lysine, which is designated P0). Yellow, H3; purple, LSD1; dashed red lines, hydrogen bonds or favorable electrostatic interactions. **(b)** The binding pocket for methylated H3-K4. **(c)** The binding pocket for Gln5, Thr6 and Ala7 of H3. **(d)** Sequence alignment of residues adjacent to known methylation sites in histones. H4, histone H4.



N terminus of H3_{1–21}K4me2 greatly diminishes its demethylation by LSD1, indicating that the active site cavity of LSD1 cannot productively accommodate more than three residues on the N-terminal side of the methyllysine.

DISCUSSION

Covalent tethering of a mechanism-based inactivator of LSD1 to FAD has allowed us to determine the structure of LSD1 bound to an H3 peptide. Our structural and biochemical studies have revealed the mechanism by which LSD1 specifically demethylates H3-K4. The H3 peptide adopts several unusual γ -turns and fits snugly into the deep catalytic cavity of LSD1, forming numerous sequence-specific interactions with LSD1. In addition, simultaneous engagement of the N terminus of H3 with the anionic pocket and the H3 methyllysine with FAD does not permit more than three residues on the N-terminal side of the methyllysine. These two effects collectively explain the H3-K4 specificity of LSD1.

Several lines of evidence indicate that the substrate-binding mode of LSD1 observed in this study using the suicide inactivator is relevant. First, our structure reveals an elegant mode of molecular recognition of the H3 tail by LSD1 and provides a straightforward explanation for the H3-K4 substrate specificity of LSD1. Second, the covalent tether between FAD and H3-K4 is a flexible alkyl chain and can allow a favorable conformation to be achieved. This flexible linker is unlikely to introduce energetic restraints that appreciably alter the binding of H3. Third, the suicide inhibitor used in this study is a mechanism-based inactivator of LSD1, and its binding mode is expected to closely resemble that of the natural substrate during catalysis. Finally, and most importantly, extensive mutagenesis studies on both LSD1 and the H3 peptide are highly consistent with the H3-binding mode observed in our structure. We emphasize that the mutagenesis studies on H3 were done with a dimethyl-Lys4-containing H3 peptide, a natural substrate of LSD1. In particular, addition of a single acetyl group at the N terminus of the H3 peptide or replacement of the N-terminal amino group with a methyl group greatly diminished its demethylation by LSD1. The large effects of these subtle changes on a natural LSD1 substrate are consistent with the substrate-binding mode of LSD1 revealed by our structure. Additional studies are needed to confirm that LSD1 indeed uses this H3-binding mode to recognize its substrate during catalysis in solution.

Our structure also provides a valuable model for the design of potent specific LSD1 inhibitors. In particular, propargylamine-containing cyclic peptidomimetics that mimic the highly compacted γ -turn conformation of the LSD1-bound H3 are expected to minimize the entropy loss upon binding to LSD1 and to inhibit LSD1 with high potency. LSD1 is a component of several transcriptional repressor complexes that also contain histone deacetylases (HDACs)^{17–20}. HDAC inhibitors have been shown to have antitumor activities²¹. Therefore, small-molecule inhibitors of LSD1 may also have therapeutic potential in treating human cancers and may have synergistic effects with HDAC inhibitors.

METHODS

Crystallization, data collection and structure determination. The complex of N-terminally truncated human LSD1 (residues 171–852) with a C-terminal fragment of CoREST (residues 286–482), termed LSD1 Δ N–CoREST–C, was purified as described⁸. The synthesis of N-methylpropargyl-K4 H3_{1–21} (a mechanism-based inactivator of LSD1 containing the N-terminal 21 residues of histone H3 and N-methylpropargyl-Lys4) and the characterization of its inhibition of LSD1 are described in the **Supplementary Methods** online. N-methylpropargyl-K4 H3_{1–21} was added to the purified LSD1 Δ N–CoREST–C

complex to a final concentration of 0.5 mM. After incubation on ice for 40 min, sodium borohydride was added to a final concentration of 1 mg ml^{–1}. Crystals of the complex were generated essentially as described⁸ with a modification to the crystallization solution, which consisted of 2 M sodium formate, 0.4 M sodium chloride, 0.1 M sodium citrate (pH 5.6) and 10 mM DTT. For cryoprotection, the crystals were incubated with crystallization solution supplemented with 23% (v/v) glycerol and then flash-cooled in liquid propane. Diffraction data were collected at beamlines 19-BM/ID (SBC-CAT) at the Advanced Photon Source (Argonne National Laboratory) and processed with HKL2000 (ref. 22). The LSD1 Δ N–CoREST–C–H3 crystals showed substantial anisotropy, with diffraction to a Bragg spacing (d_{\min}) of about 2.6 Å along the *b* and *c* axes, but to only about 3.1 Å along the *a* axis, resulting in somewhat lower completeness at the high-resolution limit. Crystals had the symmetry of space group *I*222, with cell dimensions of *a* = 120 Å, *b* = 179 Å and *c* = 235 Å, and contained one complex per asymmetric unit and 82% solvent.

The structure of the LSD1 Δ N–CoREST–C–H3 complex was determined by difference Fourier methods using the structure of the LSD1 Δ N–CoREST–C complex (PDB 2IW5) as starting model with water molecules and FAD removed. Refinement was carried out with REFMAC5 (ref. 23) from the CCP4 package²⁴, interspersed with manual rebuilding using Coot²⁵. After refinement of the LSD1 Δ N and CoREST–C proteins was complete, there was clear electron density showing binding of the H3 peptide to the LSD1 active site. The electron density indicated that the side chain of the modified H3-K4 was covalently attached to the N5 nitrogen atom of the FAD isoalloxazine ring. We modeled this adduct in accordance with the deduced chemical structure of the covalent adduct between FAD and propargyl-K4 H3_{1–21} (ref. 14). The electron density was sufficient to model the seven N-terminal residues of the peptide. There was additional weak electron density beyond Ala7 of H3, but the direction of the main chain was ambiguous, and no residues on the C-terminal side of Ala7 were included in the final model. Finally, water molecules, chloride ions and a glycerol molecule were added. The stereochemistry of the model was validated with Molprobity²⁶, which indicated that 97.1% and 2.8% of all

Table 1 Data collection and refinement statistics

	LSD1–CoREST–H3
Data collection	
Space group	<i>I</i> 222
Cell dimensions	
<i>a</i> , <i>b</i> , <i>c</i> (Å)	119.8, 178.6, 234.9
Resolution (Å)	48.57–2.72 (2.74–2.72)
<i>R</i> _{sym}	5.3 (68.1)
<i>I</i> / σ <i>I</i>	36.6 (1.8)
Completeness (%)	99.9 (98.5)
Redundancy	9.9 (8.3)
Refinement	
Resolution (Å)	48.0–2.72
No. reflections	66,383
<i>R</i> _{work} / <i>R</i> _{free}	24.19 / 27.12
No. atoms	
Protein	6,300
Ligand/ion	118
Water	51
<i>B</i> -factors (Å ²)	
Protein	75.2
Ligand/ion	82.4
Water	59.3
R.m.s. deviations	
Bond lengths (Å)	0.008
Bond angles (°)	1.205

One crystal was used for structure determination (by difference Fourier methods) and refinement. Values in parentheses are for highest-resolution shell.

residues were in the favored and allowed region of the Ramachandran plot, respectively. Gln5 of H3 is the only residue in the disallowed region, which could be due to the unusual backbone conformation in this region. The model was then verified against a simulated-annealing composite-omit map, calculated with CNS²⁷. The final model contains residues 173–836 of LSD1ΔN, residues 308–440 of CoREST-C, the covalent FAD-H3 peptide (residues 1–7) adduct, 51 water molecules, two chloride ions and one glycerol molecule. The mean *B*-values for LSD1–CoREST and the FAD-H3 adduct are 77.9 Å² and 89.3 Å², respectively, which is consistent with the Wilson *B*-value of 81.2 Å² for the diffraction data. Data collection and refinement statistics are listed in Table 1.

Demethylase assays. Expression and purification of LSD1 mutant proteins are described in **Supplementary Methods**. Initial velocity was measured using a peroxidase-coupled assay, which monitors hydrogen peroxide production as described¹⁵. The time courses of the reaction were measured under aerobic conditions using a Beckman Instruments DU series 600 spectrophotometer having a cell holder equipped with a thermostat (*T* = 25 °C). The reactions were initiated by adding 50 μl of buffered substrate solution (final concentration of H3_{1–21}K4me2 = 30–1,000 μM) to reaction mixtures (100 μl) consisting of 50 mM HEPES buffer (pH 7.5), 0.1 mM 4-aminoantipyrine, 1 mM 3,5-dichloro-2-hydroxybenzenesulfonic acid, 0.76 μM horseradish peroxidase (Worthington Biochemical Corporation) and 100–1,000 nM LSD1. Reaction mixtures were equilibrated at 25 °C for 2 min before activity measurement. Absorbance changes were monitored at 515 nm, and an extinction coefficient of 26,000 M⁻¹ cm⁻¹ was used to calculate product formation. Under these conditions, our wild-type GST-LSD1 had a *k*_{cat} of 3.1 ± 0.1 min⁻¹ and a *K*_m for H3_{1–21}K4me2 of 39 ± 2 μM.

Accession codes. Protein Data Bank: Coordinates and structure factors have been deposited with accession code 2UXN.

Note: Supplementary information is available on the Nature Structural & Molecular Biology website.

ACKNOWLEDGMENTS

Results shown in this report are derived from work performed at Argonne National Laboratory, Structural Biology Center, at the Advanced Photon Source. Argonne is operated by UChicago Argonne, LLC, for the US Department of Energy, Office of Biological and Environmental Research. This work was supported in part by grants from the US National Institutes of Health (to P.A.C.), the W.M. Keck Foundation (to H.Y.), the Welch Foundation (to H.Y.) and the Leukemia and Lymphoma Society (to H.Y.).

COMPETING INTERESTS STATEMENT

The authors declare no competing financial interests.

Published online at <http://www.nature.com/nsmb/>

Reprints and permissions information is available online at <http://npg.nature.com/reprintsandpermissions>

- Martin, C. & Zhang, Y. The diverse functions of histone lysine methylation. *Nat. Rev. Mol. Cell Biol.* **6**, 838–849 (2005).
- Ruthenburg, A.J., Allis, C.D. & Wysocka, J. Methylation of lysine 4 on histone H3: intricacy of writing and reading a single epigenetic mark. *Mol. Cell* **25**, 15–30 (2007).
- Shi, Y. *et al.* Histone demethylation mediated by the nuclear amine oxidase homolog LSD1. *Cell* **119**, 941–953 (2004).
- Shi, Y. & Whetstone, J.R. Dynamic regulation of histone lysine methylation by demethylases. *Mol. Cell* **25**, 1–14 (2007).
- Metzger, E. *et al.* LSD1 demethylates repressive histone marks to promote androgen-receptor-dependent transcription. *Nature* **437**, 436–439 (2005).
- Wissmann, M. *et al.* Cooperative demethylation by JMJD2C and LSD1 promotes androgen receptor-dependent gene expression. *Nat. Cell Biol.* **9**, 347–353 (2007).
- Garcia-Bassets, I. *et al.* Histone methylation-dependent mechanisms impose ligand dependency for gene activation by nuclear receptors. *Cell* **128**, 505–518 (2007).
- Yang, M. *et al.* Structural basis for CoREST-dependent demethylation of nucleosomes by the human LSD1 histone demethylase. *Mol. Cell* **23**, 377–387 (2006).
- Stavropoulos, P., Blobel, G. & Hoelz, A. Crystal structure and mechanism of human lysine-specific demethylase-1. *Nat. Struct. Mol. Biol.* **13**, 626–632 (2006).
- Chen, Y. *et al.* Crystal structure of human histone lysine-specific demethylase 1 (LSD1). *Proc. Natl. Acad. Sci. USA* **103**, 13956–13961 (2006).
- Banerjee, A., Yang, W., Karplus, M. & Verdine, G.L. Structure of a repair enzyme interrogating undamaged DNA elucidates recognition of damaged DNA. *Nature* **434**, 612–618 (2005).
- Zhang, X., Gureasko, J., Shen, K., Cole, P.A. & Kuriyan, J. An allosteric mechanism for activation of the kinase domain of epidermal growth factor receptor. *Cell* **125**, 1137–1149 (2006).
- Culhane, J.C. *et al.* A mechanism-based inactivator for histone demethylase LSD1. *J. Am. Chem. Soc.* **128**, 4536–4537 (2006).
- Szewczuk, L.M. *et al.* Mechanistic analysis of a suicide inactivator of histone demethylase LSD1. *Biochemistry* (in the press).
- Fornieris, F., Binda, C., Vanoni, M.A., Battaglioli, E. & Mattevi, A. Human histone demethylase LSD1 reads the histone code. *J. Biol. Chem.* **280**, 41360–41365 (2005).
- Zhang, X. *et al.* Structural basis for the product specificity of histone lysine methyltransferases. *Mol. Cell* **12**, 177–185 (2003).
- Hakimi, M.A., Dong, Y., Lane, W.S., Speicher, D.W. & Shiekhhattar, R. A candidate X-linked mental retardation gene is a component of a new family of histone deacetylase-containing complexes. *J. Biol. Chem.* **278**, 7234–7239 (2003).
- Humphrey, G.W. *et al.* Stable histone deacetylase complexes distinguished by the presence of SANT domain proteins CoREST/kiaa0071 and Mta-L1. *J. Biol. Chem.* **276**, 6817–6824 (2001).
- Shi, Y. *et al.* Coordinated histone modifications mediated by a CtBP co-repressor complex. *Nature* **422**, 735–738 (2003).
- Lee, M.G. *et al.* Functional interplay between histone demethylase and deacetylase enzymes. *Mol. Cell Biol.* **26**, 6395–6402 (2006).
- Bolden, J.E., Peart, M.J. & Johnstone, R.W. Anticancer activities of histone deacetylase inhibitors. *Nat. Rev. Drug Discov.* **5**, 769–784 (2006).
- Otwinowski, Z. & Minor, W. Processing X-ray diffraction data collected in oscillation mode. *Methods Enzymol.* **276**, 307–326 (1997).
- Murshudov, G.N., Vagin, A.A. & Dodson, E.J. Refinement of macromolecular structures by the maximum-likelihood method. *Acta Crystallogr. D Biol. Crystallogr.* **53**, 240–255 (1997).
- Collaborative Computational Project, Number 4. The CCP4 suite: programs for protein crystallography. *Acta Crystallogr. D Biol. Crystallogr.* **50**, 760–763 (1994).
- Emsley, P. & Cowtan, K. Coot: model-building tools for molecular graphics. *Acta Crystallogr. D Biol. Crystallogr.* **60**, 2126–2132 (2004).
- Lovell, S.C. *et al.* Structure validation by Ca geometry: φ, ψ and Cβ deviation. *Proteins* **50**, 437–450 (2003).
- Brünger, A.T. *et al.* Crystallography & NMR system: a new software suite for macromolecular structure determination. *Acta Crystallogr. D Biol. Crystallogr.* **54**, 905–921 (1998).